PHYSICAL REVIEW B **84**, 220401(R) (2011)

Quantum transport of two-dimensional Dirac fermions in $SrMnBi_2$

Kefeng Wang (王克锋),[1] D. Graf,[2] Hechang Lei (雷和畅),[1] S. W. Tozer,[2] and C. Petrovic[1]
[1]*Condensed Matter Physics and Materials Science Department, Brookhaven National Laboratory, Upton, New York 11973, USA*
[2]*National High Magnetic Field Laboratory, Florida State University, Tallahassee, Florida 32306-4005, USA*
(Received 3 August 2011; revised manuscript received 17 October 2011; published 1 December 2011)

We report two-dimensional quantum transport in $SrMnBi_2$ single crystals. The linear energy dispersion leads to unusual nonsaturated linear magnetoresistance since all Dirac fermions occupy the lowest Landau level in the quantum limit. The transverse magnetoresistance exhibits a crossover at a critical field B^* from semiclassical weak-field B^2 dependence to the high-field linear-field dependence. With an increase in temperature, the critical field B^* increases and the temperature dependence of B^* satisfies the quadratic behavior which is attributed to the Landau-level splitting of the linear energy dispersion. The effective magnetoresistant mobility $\mu_{MR} \sim 3400\ cm^2/V\,s$ is derived. Angular-dependent magnetoresistance and quantum oscillations suggest dominant two-dimensional (2D) Fermi surfaces. Our results illustrate the dominant 2D Dirac fermion states in $SrMnBi_2$ and imply that bulk crystals with Bi square nets can be used to study low-dimensional electronic transport commonly found in 2D materials such as graphene.

DOI: 10.1103/PhysRevB.84.220401 PACS number(s): 75.47.Np, 72.20.My, 72.80.Ga

Dirac fermions have raised great interest in condensed-matter physics, as seen by the examples of materials such as graphene[1] and topological insulators (TIs).[2] The linear dispersion between momentum and energy of Dirac fermions brings forth some interesting properties, such as zero effective mass and large transport mobility.[1,2] In addition to the surface and interface states in TIs and graphene, Dirac states in bulk materials were discussed in organic conductors[3] and iron-based superconductors such as $BaFe_2As_2$.[4,5] Recently, highly anisotropic Dirac states were observed in $SrMnBi_2$,[6,7] where linear energy dispersion originates from the crossing of two Bi $6p_{x,y}$ bands in double-sized Bi square nets. $SrMnBi_2$ has a crystal structure similar to that of the superconducting Fe pnictides and is a bad metal.[7,8] The Fermi velocity along the Γ-M symmetry line is $v_F^{\parallel} \approx 1.51 \times 10^6$ m/s, whereas the Fermi velocity in the orthogonal direction experiences a nearly one order of magnitude decrease.[7,8]

One of the interesting properties of Dirac materials is quantum transport phenomena.[9,10] Unlike the conventional electron gas with parabolic energy dispersion, where Landau levels (LLs) are equidistant,[11] the distance between the lowest and first LLs of Dirac fermions in a magnetic field is very large, and the quantum limit where all of the carriers occupy only the lowest LL is easily realized under moderate fields.[12,13] Consequently some quantum transport phenomena such as the quantum Hall effect and large linear magnetoresistance (MR) could be observed by conventional experimental methods in a Dirac fermion system.[14–17]

Here we show two-dimensional (2D) quantum transport in bulk $SrMnBi_2$ single crystals. The linear energy dispersion leads to unusual nonsaturated linear MR since all Dirac fermions occupy the lowest LL in the quantum limit. The transverse MR exhibits a crossover at a critical field B^* from the semiclassical weak-field MR $\sim B^2$ to the high-field MR $\sim B$ dependence. The critical field B^* increases with an increase in temperature, and its temperature dependence satisfies quadratic behavior which is attributed to the Landau-level splitting of the linear energy dispersion. Angular-dependent MR and oscillation indicates quasi-2D Fermi surfaces (FSs). We derive the effective magnetoresistant mobility $\mu_{MR} \sim 3400\ cm^2/V\,s$. Our results illustrate the dominant 2D Dirac fermion states in $SrMnBi_2$.

Single crystals of $SrMnBi_2$ were grown using a self-flux method.[18] Stoichiometric mixtures of Sr (99.99%), Mn (99.9%), and excess Bi (99.99%) with a ratio of Sr : Mn : Bi = 1 : 1 : 9 were sealed in a quartz tube, heated to 1050 °C, and cooled to 450 °C, where the crystals were decanted. X-ray diffraction (XRD) data were taken with Cu $K\alpha$ ($\lambda = 0.15418$ nm) radiation of a Rigaku Miniflex powder diffractometer. Transport measurements were conducted in a Quantum Design Physical Property Measurement System (PPMS-9) with a conventional four-wire method. The crystal was cleaved to a rectangular shape with dimensions of $4 \times 1\ mm^2$ in the ab plane and 0.2-mm thickness along the c axis. For in-plane resistivity $\rho_{ab}(T)$, the current path was in the ab plane, whereas the magnetic field was perpendicular to the current and parallel to the c axis, except in the rotator experiments. The c-axis resistivity $\rho_c(T)$ was measured by attaching current and voltage wires to opposite sides of the platelike crystals.[19] High-field MR oscillation was performed at the National High Magnetic Field Laboratory in the same configuration as the in-plane MR.

All powder and single-crystal XRD reflections can be indexed in the $I4/mmm$ space group by RIETICA software [Fig. 1(a)].[20] The determined lattice parameters are $a = b = 0.4561(8)$ nm and $c = 2.309(6)$ nm, in agreement with the published data.[6] The in-plane resistivity $\rho_{ab}(T)$ shown in Fig. 1(b) exhibits a metallic behavior. An external magnetic field enhances the resistivity. As the temperature is increased, MR is gradually suppressed and is rather small above ~60 K. Resistivity along the c axis [$\rho_c(T)$] is nearly two orders of magnitude larger than $\rho_{ab}(T)$ and exhibits a weak crossover at high temperature. In what follows we will discuss in-plane MR.

Angular-dependent MR $\rho(B,\theta)$ at $T \sim 2$ K is shown in Figs. 2(a) and 2(b). The crystal was mounted on a rotating stage such that the tilt angle θ between the sample surface (ab plane) and the magnetic field can be continuously changed, with currents flowing in the ab plane perpendicular to the magnetic field [the inset in Fig. 2(a)]. The magnetoresistance of

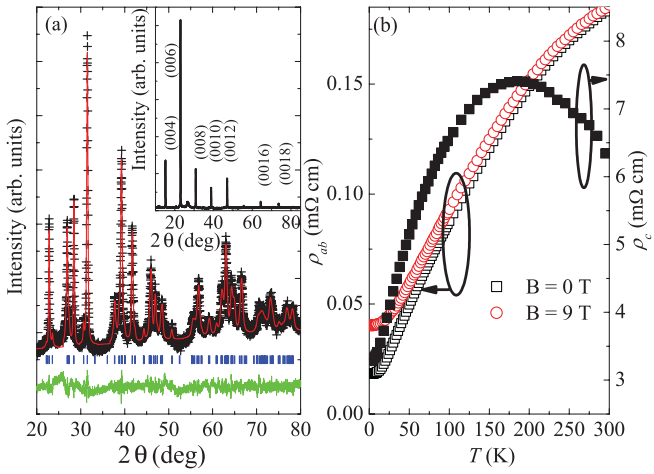

FIG. 1. (Color online) (a) Powder XRD patterns and structural refinement results. The data were shown by (+), and the fit is given by the red (gray) solid line. The difference curve (the green/light gray solid line) is offset. The inset shows the single-crystal XRD pattern indicating the c-axis orientation of crystal. (b) Temperature dependence of the in-plane resistivity $\rho_{ab}(T)$ (open symbols) and c-axis resistivity $\rho_c(T)$ (filled symbols) in $B = 0$ T (squares) and $B = 9$ T (circles) magnetic fields, respectively.

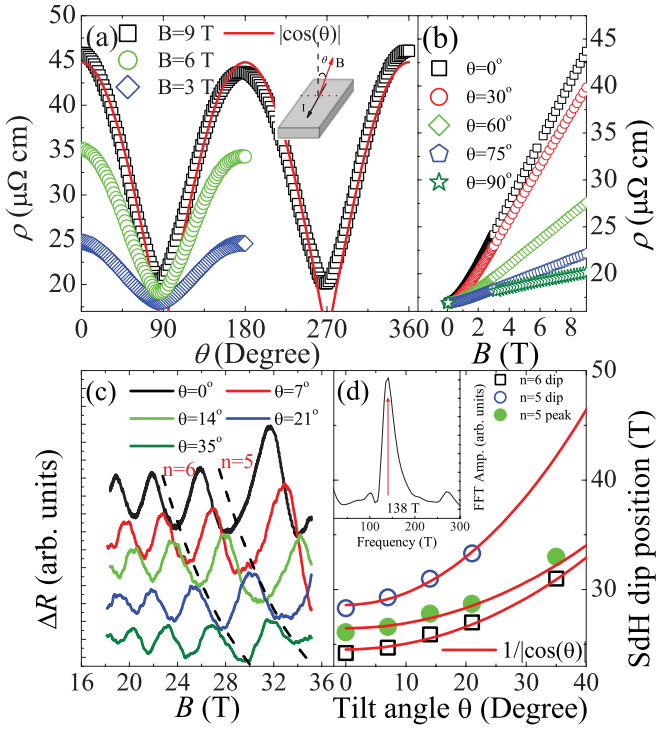

FIG. 2. (Color online) (a) In-plane resistivity ρ vs the tilt angle θ from 0° to 360° at $B = 3$, 6, and 9 T and $T = 2$ K. The red line is the fitting curve using $|\cos(\theta)|$ (see text). The inset shows the configuration of the measurement. (b) In-plane resistivity ρ vs magnetic field B with different tilt angles θ at 2 K. (c) MR SdH oscillations $\Delta R = R_{xx} - \langle R \rangle$ as a function of field B below 35 T with tilt angles θ from 0° to 35° at 2 K. The dashed lines indicate the SdH dips at a Landau filling factor of $\upsilon = 5$ and 6. The different curves are offset for clarification. (d) Position of dips with $\upsilon = 5$ and 6, as well as the position of peaks with $\upsilon = 5$, plotted against the tilt angle θ. The data are consistent with the $1/|\cos(\theta)|$ dependence (red lines). The inset shows the Fourier transform of the SdH oscillation, which gives a single frequency of $F = 138(7)$ T.

$SrMnBi_2$ exhibits a significant angular dependence [Figs. 2(a) and 2(b)]. When B is parallel to the c axis ($\theta = 0°$), the MR is maximized and is linear above a characteristic field (~1 T). With an increase in the tilt angle θ, MR gradually decreases and becomes nearly negligible for B in the ab plane ($\theta = 90°$).

The response of the carriers to the applied magnetic field and the magnitude of MR is determined by the mobility in the plane perpendicular to the magnetic field.[11] For nearly isotropic three-dimensional (3D) FSs, there should be no significant angle-dependent MR (AMR). In (quasi-)2D systems, 2D states will only respond to a perpendicular component of the magnetic field $B|\cos(\theta)|$, and consequently longitudinal AMR and AMR oscillation were observed in some quasi-2D conductors [such as Sr_2RuO_4 and β-(BEDT-TTF)$_2I_3$] and the surface states of TIs.[14,15,21,22] For example, the MR of the bulk state in a topological insulator has only ~10% angular dependence while the angular dependence of MR in the surface state is approximately ten times larger.[15] Significant AMR was also observed in some materials with highly anisotropic 3D FSs such as Bi and Cu, but the period of AMR is determined by the shape of the Fermi surface and is very different from the one in 2D systems. In Bi, electrons exhibit a threefold valley degeneracy and in-plane mass anisotropy, so the AMR peaks each time when the magnetic field is oriented along the bisectrix axis and has a 60° period.[23] In Cu the AMR is more complex due to the complex FSs and peaks approximately every 25°.[24]

The electronic structure calculations in $SrMnBi_2$ show that the states near the Fermi energy E_F are dominated by the Bi states in the Bi square nets. Consequently the dominant FS should be quasi-2D. Angular-dependent resistivity in $B =$ 9 T and $T = 2$ K shows wide maximum when the field is parallel to the c axis ($\theta = 0°, 180°$), and a sharper minimum at approximately $\theta = 90°, 270°$ [Fig. 2(a)]. The whole curve of AMR in $SrMnBi_2$ follows the function of $|\cos(\theta)|$ very well with a 180° period [red line in Fig. 2(a)]. Moreover, the larger ρ_c than ρ_{ab} in Fig. 1(b) implies that the transfer integral and the coupling between layers along the c axis is very small. All this implies that the FSs in $SrMnBi_2$ should be highly anisotropic and that the mobility of carriers along k_z is much smaller than the value in the k_xk_y plane.

Angular-dependent MR quantum oscillations are directly related to the cross section of FS. In Fig. 2(c), the in-plane $\Delta R = R - \langle R \rangle$ measured using the same configuration as shown in the inset of Fig. 2(a) exhibits clear Shubnikov–de Haas (SdH) oscillations with tilt angles θ from 0° to 35°. In metals, SdH oscillations correspond to successive emptying of LLs by the magnetic field and the LL index n is related to the cross section of FS S_F by $2\pi(n + \gamma) = S_F \frac{\hbar}{eB}$.[14,15,25] For a 2D FS (a cylinder), the cross section has $S_F(\theta) = S_0/|\cos(\theta)|$ angular dependence and the LL positions should be inversely proportional to $|\cos(\theta)|$.[14,25] The peak (dip) positions in $SrMnBi_2$ rapidly shift toward a higher-field direction with an increase in θ [as indicated by the dashed lines in Fig. 2(c)]. In Fig. 2(d), the dip positions corresponding to LLs $n = 5,6$ and the peak position with $n = 5$ were plotted against the tilt angle

θ and can be described very well by $1/|\cos(\theta)|$ [the red lines in Fig. 2(d)]. Similar behavior was observed in the surface states of TIs[14,15] and some other layered structures.[25,26] The Fourier transform of the SdH oscillation [the inset of Fig. 2(d)] revealed that the oscillation component shows a periodic behavior in $1/B$ with a single frequency $F = 138(7)$ T. The small value of frequency is consistent with the previous value given in Ref. 7 and demonstrates that the dominant FSs are very small since the Onsager relation is $F = (\Phi_0/2\pi^2)A_k$, where Φ_0 is the flux quantum and A_k is the cross-sectional area of the FS.[25] This clearly shows that the dominant two-dimensional FSs found in Fig. 2(b) are indeed the small FSs between the Γ and M points, rather than the large FSs at the Γ point in the Brillouin zone. Above SdH oscillation combined with the angular MR clearly suggests that the dominant FSs of $SrMnBi_2$ are small quasi-2D cylinders along k_z, originating from Bi square nets. In addition, there are still conventional parabolic bands with three-dimensional characteristics close to the Fermi level,[7] causing a small deviation from quasi-2D transport.

Now we turn to the linear nonsaturated in-plane magnetoresistance in $SrMnBi_2$ [Fig. 3(a)]. The MR is linear over a wide field range up to 50 K. This behavior extends to very low fields where the MR naturally reduces to a weak-field semiclassical quadratic dependence. The crossover from the weak-field B^2 dependence to the high-field linear dependence can best be seen by considering the field derivative of the MR, $d\mathrm{MR}/dB$ [Fig. 3(b)]. In the low-field range ($B < 1$ T at 2 K), $d\mathrm{MR}/dB$ is proportional to B (as shown by the lines in the low-field regions), indicating the semiclassical $\mathrm{MR} \sim A_2B^2$. But above a characteristic field B^*, $d\mathrm{MR}/dB$ deviates from the semiclassical behavior and saturates to a much reduced slope (as shown by the lines in the high-field region). This indicates that the MR for $B > B^*$ is dominated by a linear field dependence plus a very small quadratic term [$\mathrm{MR} = A_1B + O(B^2)$].

The linear MR deviates from the semiclassical B^2 dependence of MR in the low-field region and a saturating MR in high fields.[11] The unusual nonsaturating linear magnetoresistance has been reported in the gapless semiconductor $Ag_{2-\delta}(Te/Se)$ (Refs. 27 and 28) with a linear energy spectrum in the quantum limit.[10,28] Recent first-principle calculations confirmed that these materials have a gapless Dirac-type surface state.[29] Linear magnetoresistance is also observed in topological insulators[14,15] and $BaFe_2As_2$ (Ref. 16) with Dirac fermion states. Another possible origin of the large linear magnetoresistance is the mobility fluctuations in a strongly inhomogeneous system.[30] This does not apply in $SrMnBi_2$ since our sample is a stoichiometric crystal without doping and/or disorder. Below we show that the nonsaturating linear magnetoresistance and the deviation from the semiclassical transport in $SrMnBi_2$ is due to the linear energy dispersion.

The application of a strong perpendicular external magnetic field (B) would lead to a complete quantization of the orbital motion of carriers with linear energy dispersion, resulting in quantized LLs $E_n = \mathrm{sgn}(n)v_F\sqrt{2e\hbar B|n|}$, where $n = 0, \pm 1, \pm 2, \ldots$ is the LL index and v_F is the Fermi velocity.[12,13] Then the energy splitting between the lowest and first LLs is described by $\Delta_{\mathrm{LL}} = \pm v_F\sqrt{2e\hbar B}$.[12,13] In the quantum limit at a specific temperature and field, Δ_{LL} becomes larger than both the Fermi energy E_F and the thermal fluctuations k_BT at a finite temperature. Consequently all carriers occupy the lowest Landau level and eventually the quantum transport with linear magnetoresistance shows up. The critical field B^* above which the quantum limit is satisfied at a specific temperature T is $B^* = \frac{1}{2e\hbar v_F^2}(E_F + k_BT)^2$.[16] The splitting of LLs in conventional parabolic bands is $\Delta_{\mathrm{LL}} = \frac{e\hbar B}{m^*}$. Hence the evolution of Δ_{LL} with field for parabolic bands is much slower than that for Dirac fermion states, and it is difficult to observe a quantum limit behavior in the moderate-field range. The temperature dependence of critical field B^* in $SrMnBi_2$

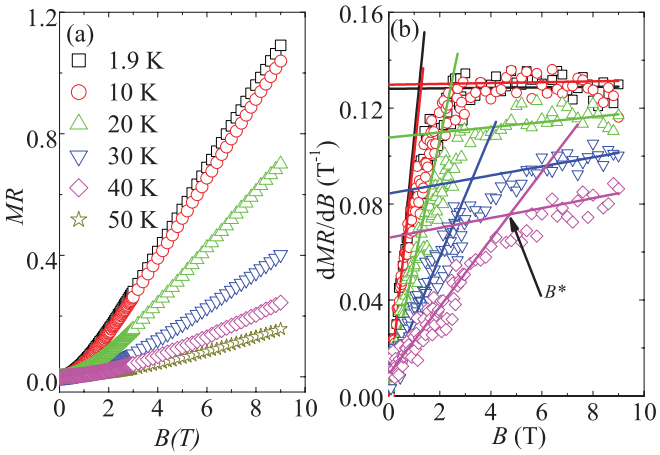

FIG. 3. (Color online) (a) The magnetic field (B) dependence of the in-plane magnetoresistance (**MR** $= [\rho(B) - \rho(0)]/\rho(0)$**)** at different temperatures. (b) The field derivative of in-plane MR at different temperatures, respectively. The lines in the high-field regions were fitting results using $\mathrm{MR} = A_1B + O(B^2)$ and the lines in low-field regions using $\mathrm{MR} = A_2B^2$.

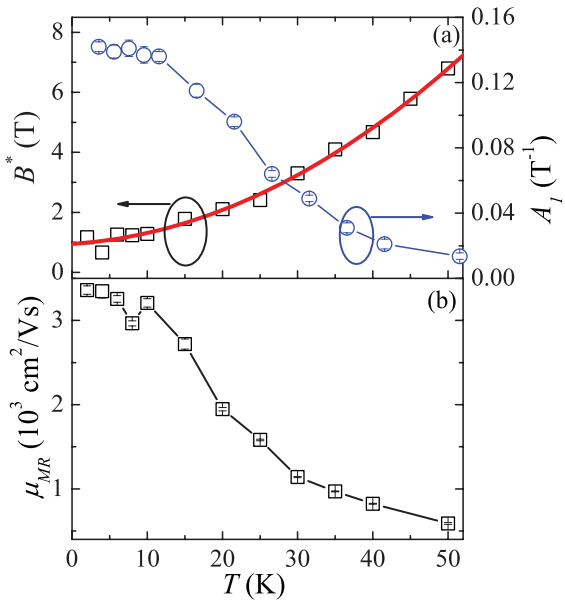

FIG. 4. (Color online) (a) Temperature dependence of the critical field B^* (black squares) and the high-field MR linear coefficient A_1 (blue circles) up to 50 K. The red solid line is the fitting results using $B^* = \frac{1}{2e\hbar v_F^2}(E_F + k_BT)^2$. (b) Temperature dependence of the effective MR mobility μ_{MR} extracted from the weak-field MR.

clearly deviates from the linear relationship and can be well fitted by $B^* = \frac{1}{2e\hbar v_F^2}(E_F + k_B T)^2$, as shown in Fig. 4(a). The fitting gives the Fermi velocity $v_F \sim 5.13 \times 10^5$ ms^{-1} and $\Delta_1 \sim 4.97$ meV. This confirms the existence of Dirac fermion states in $SrMnBi_2$.

In a multiband system with both Dirac and conventional parabolic-band carriers (including electrons and holes) the magnetoresistance in the semiclassical transport can be described as $MR = \frac{\sigma_e\sigma_h(\mu_e+\mu_h)^2}{(\sigma_e+\sigma_h)^2}B^2$, where $\sigma_e, \sigma_h, \mu_e, \mu_h$ are the effective electron and hole conductivity and mobility in zero field, respectively, when the Dirac carriers are dominant in transport.[16,17] Then the coefficient of the low-field B^2 quadratic term A_2 is related to the effective MR mobility $\sqrt{A_2} = \frac{\sqrt{\sigma_e\sigma_h}}{\sigma_e+\sigma_h}(\mu_e + \mu_h) = \mu_{MR}$, which is smaller than the average mobility of carriers $\mu_{ave} = \frac{\mu_e+\mu_h}{2}$ and gives an estimate of the lower bound. Figure 4(b) shows the dependence of μ_{MR} on the temperature. At 2 K, the value of μ_{MR} is $\sim$3400 cm^2/V s. The large effective MR mobility also implies that Dirac fermions dominate the transport behavior. With an increase in temperature, the value of μ_{MR} and the coefficient of the high-field linear term A_1 [Fig. 4(a)] decrease sharply. This is due to thermal fluctuation smearing out the LL splitting.

In summary, we demonstrate quantum transport of 2D Dirac fermion states in bulk $SrMnBi_2$ single crystals. The bands with linear energy dispersion lead to a large nonsaturated linear magnetoresistance since all Dirac fermions occupy the lowest Landau level in the quantum limit. The transverse magnetoresistance exhibits a crossover at a critical field B^* from a semiclassical weak-field B^2 dependence to a high-field linear-field dependence. With an increase in temperature, the critical field B^* increases and the temperature dependence of B^* satisfies quadratic behavior which is attributed to the Landau-level splitting of the linear energy dispersion. The effective magnetoresistant mobility $\mu_{MR} \sim 3400$ cm^2/V s, comparable to values observed in graphene, is observed. The angle dependence of magnetoresistance shows a $|\cos(\theta)|$ dependence while the LL positions in SdH oscillations are inversely proportional to $|\cos(\theta)|$, indicating dominant quasi-2D Fermi surfaces. Our results show that the crystals with Bi square nets can host phenomena commonly observed so far in 2D structures and materials such as graphene.

We than John Warren for help with SEM measurements. Work at Brookhaven is supported by the US DOE under Contract No. DE-AC02-98CH10886. Work at the National High Magnetic Field Laboratory is supported by the DOE NNSA DEFG52-10NA29659 (S.W.T and D.G.), by the NSF Cooperative Agreement No. DMR-0654118, and by the state of Florida.

[1] A. H. Castro Neto, F. Guinea, N. M. R. Reres, K. S. Novoselov, and A. K. Geim, Rev. Mod. Phys. **81**, 109 (2009).
[2] M. Z. Hasan and C. L. Kane, Rev. Mod. Phys. **82**, 3045 (2010).
[3] N. Tajima, S. Sugawara, R. Kato, Y. Nishio, and K. Kajita, Phys. Rev. Lett. **102**, 176403 (2009).
[4] P. Richard, K. Nakayama, T. Sato, M. Neupane, Y.-M. Xu, J. H. Bowen, G. F. Chen, J. L. Luo, N. L. Wang, X. Dai, Z. Fang, H. Ding, and T. Takahashi, Phys. Rev. Lett. **104**, 137001 (2010).
[5] T. Morinari, E. Kaneshita, and T. Tohyama, Phys. Rev. Lett. **105**, 037203 (2010).
[6] G. Cordier and H. Schaffer, Z. Naturforsch. B **32**, 383 (1977).
[7] J. Park, G. Lee, F. Wolff-Fabris, Y. Y. Koh, M. J. Eom, Y. K. Kim, M. A. Farhan, Y. J. Jo, C. Kim, J. H. Shim, and J. S. Kim, Phys. Rev. Lett. **107**, 126402 (2011).
[8] J. K. Wang, L. L. Zhao, Q. Yin, G. Kotliar, M. S. Kim, M. C. Aronson, and E. Morosan, Phys. Rev. B **84**, 064428 (2011).
[9] H. A. Yang, B. Fauque, L. Malone, A. B. Antunes, Z. W. Zhu, C. Uher, and K. Behnia, Nat. Commun. **1**, 47 (2011).
[10] A. A. Abrikosov, Phys. Rev. B **58**, 2788 (1998).
[11] A. A. Abrikosov, *Fundamentals of the Theory of Metals* (North-Holland, Amsterdam, 1988).
[12] Y. Zhang, Z. Jiang, Y.-W. Tan, H. L. Stormer, and P. Kim, Nature (London) **438**, 201 (2005).
[13] D. Miller, K. Kubista, G. Rutter, M. Ruan, W. de Heer, P. First, and J. Stroscio, Science **324**, 924 (2009).
[14] D.-X. Qu, Y. S. Hor, J. Xiong, R. J. Cava, and N. P. Ong, Science **329**, 821 (2010).
[15] J. G. Analytis, R. D. McDonald, S. C. Riggs, J.-H. Chu, G. S. Boebinger, and I. R. Fisher, Nat. Phys. **6**, 960 (2010).
[16] K. K. Huynh, Y. Tanabe, and K. Tanigaki, Phys. Rev. Lett. **106**, 217004 (2011).
[17] H.-H. Kuo, J.-H. Chu, S. C. Riggs, L. Yu, P. L. McMahon, K. DeGreve, Y. Yamamoto, J. G. Analytis, and I. R. Fisher, Phys. Rev. B **84**, 054540 (2011).
[18] P. C. Canfield and Z. Fisk, Philos. Mag. B **65**, 1117 (1992).
[19] X. F. Wang, T. Wu, G. Wu, H. Chen, Y. L. Xie, J. J. Ying, Y. J. Yan, R. H. Liu, and X. H. Chen, Phys. Rev. Lett. **102**, 117005 (2009).
[20] B. Hunter, "RIETICA—A Visual RIETVELD Program," International Union of Crystallography Commission on Powder Diffraction Newsletter No. 20 (Summer), 1998 [http://www.rietica.org].
[21] E. Ohmichi, H. Ito, T. Ishiguro, T. Komatsu, and G. Saito, J. Phys. Soc. Jpn. **66**, 310 (1997).
[22] E. Ohmichi, H. Adachi, Y. Mori, Y. Maeno, T. Ishiguro, and T. Oguchi, Phys. Rev. B **59**, 7263 (1999).
[23] Z. Zhu, A. Collaudin, B. Fauque, W. Kang, and K. Behnia, Nat. Phys. doi: 10.1038/nphys2111 (2011).
[24] J. R. Klauder, W. A. Reed, G. F. Brennert, and J. E. Kunzler, Phys. Rev. **141**, 592 (1966).
[25] D. Shoenberg, *Magnetic Oscillations in Metals* (Cambridge University Press, Cambridge, UK, 1984).
[26] A. I. Coldea, J. D. Fletcher, A. Carrington, J. G. Analytis, A. F. Banagura, J.-H. Chu, A. S. Erickson, I. R. Fisher, N. E. Hussey, and R. D. McDonald, Phys. Rev. Lett. **101**, 216402 (2008).
[27] R. Xu, A. Husmann, T. F. Rosenbaum, M.-L. Saboungi, J. E. Enderby, and P. B. Littlewood, Nature (London) **390**, 57 (1997).
[28] M. Lee, T. F. Rosenbaum, M.-L. Saboungi, and H. S. Schnyders, Phys. Rev. Lett. **88**, 066602 (2002).
[29] W. Zhang, R. Yu, W. Feng, Y. Yao, H. Weng, X. Dai, and Z. Fang, Phys. Rev. Lett. **106**, 156808 (2011).
[30] M. M. Parish and P. B. Littlewood, Nature (London) **426**, 162 (2003).